

STRUCTURE OF ALKALI BIPHENYL ION PAIRS IN SOLUTION AND IN THE SOLID STATE

E. de Boer, A.A.K. Klaassen, J.J. Mooij and J.H. Noordik

Research Institute of Materials (RIM), University of Nijmegen, Toernooiveld,
6525 ED NIJMEGEN, The Netherlands

Abstract - NMR experiments on sodium biphenyl (NaBp), potassium biphenyl (KBp) and rubidium biphenyl (RbBp), dissolved in various solvents are summarized with emphasis on the structural information which can be obtained from such experiments. The crystal structures of NaBp.2Tg (Tg = triglyme), KBp.2Ttg and RbBp.2Ttg (Ttg = tetraglyme) are discussed, in relation to the NMR results obtained for these systems in solution. In the solid state these crystals may be considered to be built up of solvent separated ion pairs. Magnetic experiments are reported for single crystals of the three systems. Susceptibility measurements revealed a ferromagnetic coupling in NaBp.2Tg and KBp.2Ttg and an antiferromagnetic coupling in RbBp.2Ttg. All crystals exhibit an exchange narrowed ESR line, with an orientation dependent linewidth. From the resonance positions the molecular g tensor of the biphenyl anion could be derived. The orientation dependent linewidth is due to dipolar interactions between the spins. A quantitative explanation of it could not be given at present.

INTRODUCTION

The early work of Fuoss (1954, ref. 1) and Winstein (1954, ref. 2) suggested that ion pairs may exist in solution in two different distinct forms. In later work it has become customary to refer to them as the loose or solvent separated and the tight or contact ion pairs. During the last two decades these species have been studied in great detail, using optical and magnetic resonance techniques, and also conductivity methods. Especially in numerous experiments carried out by Szwarc et al. (3) it has been shown that ion pairs are well defined chemical species with their own physical properties.

In 1970 Canters et al. (4) succeeded in preparing single crystals of the paramagnetic alkali biphenyl ion pairs. The crystal structure of one of its representatives viz. the rubidium biphenyl ion pair was recently solved at this laboratory (5). It appeared that the structure could be characterized as a solvent separated ion pair, in which the cation is completely surrounded by two tetraglyme molecules. Stucky et al. (6) reported the structures of some diamagnetic aromatic ion pairs, using tetramethylethylenediamine and bisquinuclidine as coordinating molecules. In these complexes, the cation is coordinated to the aromatic moiety and to the nitrogen atoms of the coordinating molecules, and hence these species belong to the category of contact ion pairs. Another class of interesting single crystals of diamagnetic ion pairs is formed by the alkali complexes derived from cyclooctatetraene and its derivatives (7). The crystal structures reveal that the alkali ions are located above the center of the planar eight-membered ring, at a distance of about 2.5 Å, thus showing that these crystals also belong to the class of contact ion pair structures.

In this paper we report the results of magnetic and X-ray diffraction measurements obtained on three alkali biphenyl (Bp) systems, viz. NaBp in triglyme (Tg), KBp in tetraglyme (Ttg) and RbBp in tetraglyme (Ttg). The chemical formula of Tg and Ttg is: $\text{CH}_3\text{O}(\text{CH}_2\text{CH}_2\text{O})_n\text{CH}_3$ with $n = 3$ and 4 , respectively. For all the three systems single crystals could be prepared, with composition NaBp.2Tg, KBp.2Ttg and RbBp.2Ttg. The crystal structure of NaBp.2Tg has been solved recently and has not been reported yet. In this study the results of experiments on these systems in solution and in the solid state will be discussed. Special attention will be paid to the structural parameters of the three systems in the solid state in particular to those of the NaBp system. The characteristics of the latter will be compared with those of the KBp and RbBp systems.

EXPERIMENTAL

Preparation

Solutions containing 0.5 - 1.0 M of alkali biphenyl were prepared under high vacuum using standard techniques (8). Single crystals were prepared by cooling the solutions from 30°C to 10°C, at the rate of 1°/hr. NaBp.2Tg crystallizes in rectangular shaped plates, KBp.2Ttg in cubic small plates and the crystals of RbBp.2Ttg are needles. All crystals are darkly blue colored and melt below 60°. These low melting points and the sensitivity of these crystals to air and moisture makes it necessary to carry out all manipulations in an inert atmosphere

and at a temperature of about -20°C .

Magnetic measurements

The NMR, ESR and susceptibility apparatuses, used to measure the magnetic properties of the alkali biphenyl ions, have been described elsewhere (9). For a detailed description on handling the highly air sensitive crystals we also refer to earlier publications (7,9).

Structure determinations

Crystal structures of RbBp.2Ttg (5) and KBp.2Ttg (10) have already been published. Recently we succeeded in solving the crystal structure of NaBp.2Tg. A full account of the structure determination of this compound will be given elsewhere (11). Table 1 gives the single crystal data of NaBp.2Tg along with those of KBp.2Ttg and RbBp.2Ttg for comparison purposes.

TABLE 1. Crystal data of NaBp.2Tg, KBp.2Ttg and RbBp.2Ttg

	NaBp.2Tg	KBp.2Ttg	RbBp.2Ttg
	$\text{C}_{28}\text{H}_{46}\text{O}_8\text{Na}$	$\text{C}_{32}\text{H}_{54}\text{O}_{10}\text{K}$	$\text{C}_{32}\text{H}_{54}\text{O}_{10}\text{Rb}$
Mw	533.7	565.8	621.2
	at 148 K	at 120 K	at 100 K
a	11.721(2) Å	9.654(3) Å	30.68(2) Å
b	13.425(2) Å	16.803(9) Å	9.79(1) Å
c	9.555(2) Å	21.845(7) Å	23.71(2) Å
β	103.08 (2) $^{\circ}$	96.03 (2) $^{\circ}$	103.34(6) $^{\circ}$
V	1464.5 Å ³	3465 Å ³	6909 Å ³
space group	P_{21}	C2/c	C2/c
Z	2	4	8
d_x	1.16 g/cm ³	1.03 g/cm ³	1.31 g/cm ³

NMR EXPERIMENTS ON SOLUTIONS

Solutions of alkali biphenyl ion pairs have been studied extensively with NMR by Canters and de Boer (12). From such studies one gets information about the structure of the ion pairs. This information can be inferred from the shift of the resonance lines and from the linewidths. Especially alkali NMR provides a wealth of information about the structure of ion pairs in solution as will be illustrated briefly for the three ion pair systems dealt with in this paper.

Shift of the alkali resonance lines

The Boltzmann distribution over the spin states of the paramagnetic particles ($S = \frac{1}{2}$) causes a shift, δ_c^0 , of the alkali resonance lines as given by (12)

$$\delta_c^0 \text{ (in ppm)} = \frac{-|\gamma_e|}{\gamma_N} \frac{A}{4kT} \quad (1)$$

in which A represents the Fermi contact interaction in energy units and γ_e and γ_N are the gyromagnetic ratios of electron and nucleus, respectively. A is related to the hyperfine splitting constant (hfsc), \underline{a} , known from ESR experiments by

$$A = |\gamma_e| \hbar \underline{a} \quad (2)$$

Apart from the Fermi contact shift, δ_c^0 , the experimental shift, δ_c^{exp} , may contain contributions from other interactions, among which the most important is the interaction between the electrons in the valence orbitals of the cation and the electrons in orbitals of atoms belonging to the solvation shell of the alkali ion. Consequently, δ_c^{exp} can be represented by

$$\delta_c^{\text{exp}} = \delta_c^0 + \Delta\sigma \quad (3)$$

where $\Delta\sigma$ takes into account all shift contributions other than those due to the Fermi contact interaction. It has been shown (12) that in most cases $\Delta\sigma$ is negligible with respect to δ_c^0 , so that the hfsc, \underline{a} , can be abstracted directly from the experimental shift.

In Figure 1 the results of a series of measurements are shown on NaBp dissolved in a variety of solvents. The solvents used were tetrahydrofuran (THF), dimethoxyethane (DME), diglyme (Dg), triglyme (Tg) and tetraglyme (Ttg). In Figure 2 the \underline{a} versus T plots are shown for $^{87}\text{RbBp}$ dissolved in DME, Dg and Tg.

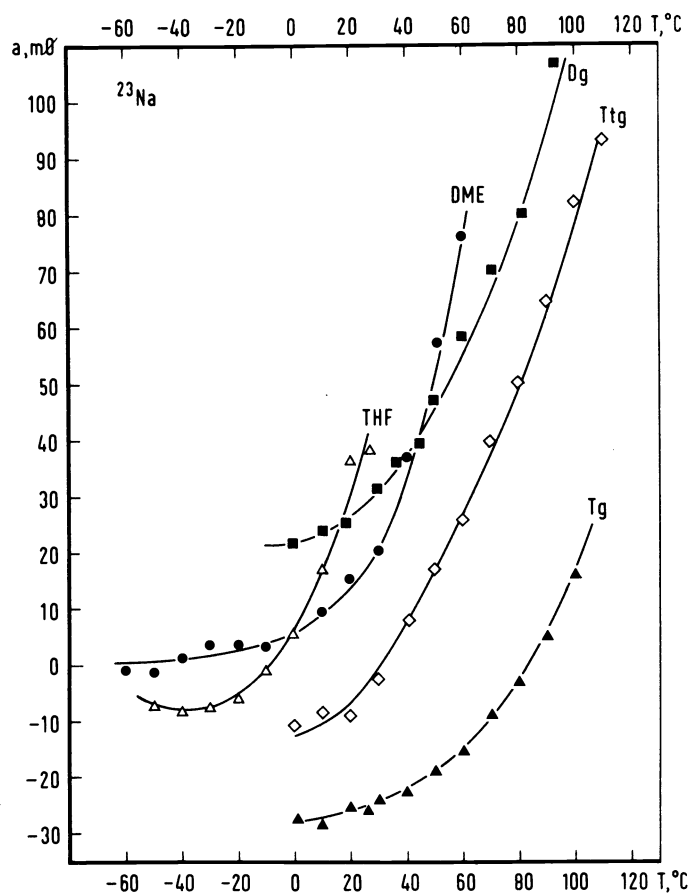


Fig. 1. ^{23}Na hfsc in $m\phi$ as a function of the temperature for solutions of NaBp in THF (1.94 M), DME (1.0 M), Dg (1.7 M), Tg (1.0 M) and Ttg (0.77 M).

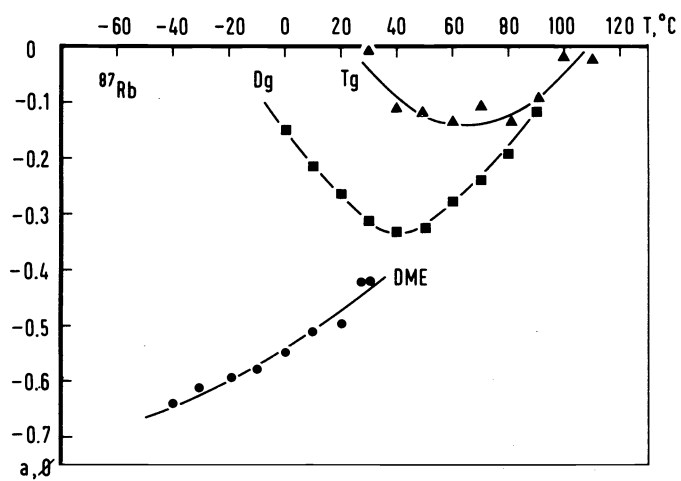


Fig. 2. ^{87}Rb hfsc in ϕ as a function of the temperature for solutions of RbBp in DME (1.50 M), Dg (1.25 M) and Tg (0.90 M).

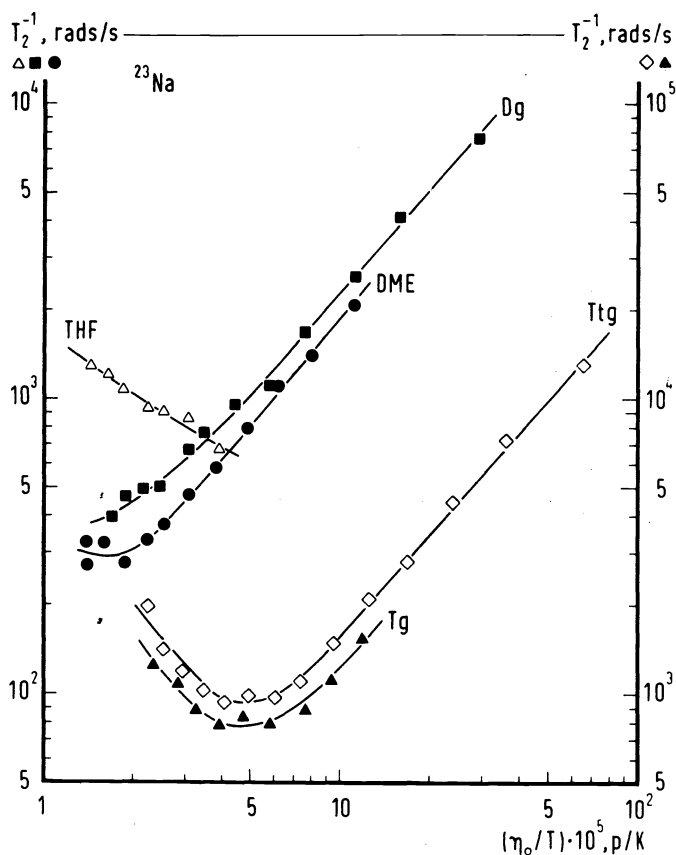


Fig. 3. ^{23}Na NMR linewidths in rad/s as a function of the viscosity of the pure solvent divided by the absolute temperature for solutions of NaBp in THF, DME, Dg, Tg and Ttg.

perature. From this one may infer that contact ion pairs exist in this solution, so that the interaction parameters can change with temperature. From the straight plots of T_2^{-1} versus η_0/T for NaBp in DME and Dg one may conclude that solvent separated ion pairs are present in solution, because only then it is conceivable that the interaction parameters do not change with temperature. Since Tg and Ttg are even better solvating agents than Dg, one expects the Na NMR linewidth in solutions of NaBp in these solvents to be proportional to η_0/T . The observed increase in T_2^{-1} at high temperatures is therefore anomalous. This, together with the earlier observed anomalous behavior of the Na shifts in these solvents suggests that a special ion pair structure prevails in these solvents at low temperatures and that at high temperatures a disruption of this structure occurs, leading to an increase of the interaction parameters and, accordingly to an increase of the linewidth.

The straight plots observed for KBp in DME, Dg, Tg and Ttg (Figure 4) point to solvent separated ion pairs. A numerical analysis of the linewidth led to the conclusion that $(T_2^{-1})_Q$ dominates the linewidth.

The linewidth plots for RbBp in DME, Dg and Tg show a similar behavior as those for KBp and therefore the same conclusion as stated for KBp applies.

(i) Temperature dependence

Going to lower temperatures the $\Delta\sigma$ versus T plots for NaBp level off to a constant value (Figure 1). From this one may conclude that the average solvation of the cations increases on going to lower temperatures causing a decrease of the Fermi contact interaction, so that finally at very low temperatures $\Delta\sigma$ dominates the shift. Noteworthy is the behavior of the curve measured in Tg. At high temperatures a low field shift is observed and at low temperatures a high field shift, both measured with respect to the reference sample of NaCl in H₂O. Since Tg is a very good solvating solvent this behavior cannot be explained by a change of sign of the hfsc, as has been observed for NaBp in tetrahydropyran (THP). However, it can be explained by assuming that NaBp in Tg forms at low temperatures a specific ion pair structure, so that large contributions to $\Delta\sigma$ arise. This may be the reason why NaBp forms single crystals only in Tg.

The almost linear increase of $\Delta\sigma$ (⁸⁷Rb) with temperature for RbBp in DME (Figure 2) indicates that contact ion pairs exist, with differing average position of the alkali ion with respect to the biphenyl anion as a function of temperature. Since the metal spin density depends on the position of the alkali ion the hfsc changes with temperature. In the better solvating solvents Dg and Tg curved plots are obtained. This can be rationalized by assuming that at a high temperature contact ion pairs exist and that by decreasing the temperature these ion pairs are converted to solvent separated ion pairs. During this process the hfsc diminishes and approaches zero. This view is supported by the fact that by extrapolating the curve for DME to high temperatures one finds that the hfsc's for Rb in the three mentioned solvents are the same.

The hfsc of K in the systems KBp, dissolved in DME, Dg, Tg and Ttg is small (between 0-20 moersted) and negative. They hardly change with temperature. These observations point to solvent separated ion pairs.

(ii) Solvent dependence

The solvating power of the solvents used increases in the order THF < DME < Dg < Tg < Ttg. One would therefore expect that at a properly chosen temperature one would observe a change in ion pair structure from contact to solvent separated going along the above mentioned series of solvents, which would result in a decrease of the value of the hfsc. Since for small hfsc's $\Delta\sigma$ may contribute considerably, the criterion for the solvating power can better be formulated in terms of the slopes of the plots: the smaller the solvating power the larger the slope at a given temperature and the lower the temperature at which a given value of the slope will be reached. This is borne out by the experimental results of NaBp, with an irregularity at the transition from Tg to Ttg. Also here a specific ion pair structure might explain this anomalous behavior.

Comparing the results of RbBp with NaBp one sees that solvent separated ion pairs are more easily formed as the radius of the cation decreases. For example NaBp forms solvent separated ion pairs in DME at low temperatures, whereas RbBp forms only contact ion pairs in this solvent (cf Figures 1 and 2).

Broadening of the alkali resonance lines

The alkali resonance lines are severely broadened by the Fermi contact, the anisotropic magnetic electron-nuclear dipolar and quadrupole relaxation. For the solutions studied the correlation times τ_c were so large that $\omega_e^2 \tau_c^2 \gg 1$, (ω_e is the Larmor frequency of the electron) and that, accordingly, only secular parts of the various relaxation mechanisms contribute dominantly to T_2^{-1} . Under the assumption that the ion pairs can be described by a static model, which means that at each temperature a well defined ion pair structure exists, the following expressions for the relevant relaxation mechanisms can be derived (12):

$$(T_2^{-1})_{Fc} = \frac{1}{4} \left(\frac{\bar{A}}{\hbar}\right)^2 \tau_e \quad (4)$$

$$(T_2^{-1})_D = \frac{7}{120} \frac{D:D}{\hbar^2} \tau_d \quad (5)$$

$$(T_2^{-1})_Q = \frac{3}{40} f(I) \left(\frac{e^2 Qq}{\hbar}\right)^2 \tau_r \quad (6)$$

in which \bar{A} is the averaged Fermi contact interaction constant, D characterizes the dipolar interaction ($D:D = \sum_{\alpha,\beta} (D_{\alpha\beta})^2$, α and β are components of r , the distance between the un-

paired electron and the nucleus), eQ is the quadrupole moment, eq the electric field gradient (for simplicity reasons it is assumed that the quadrupole tensor has axial symmetry), and $f(I)$ is equal to $2I + 3/I^2(2I - 1)$. The correlation times τ_e , τ_d and τ_r are all proportional to η/T , provided Eq.(4-6) are valid.

In Figure 3 and Figure 4 the linewidths are plotted versus the viscosity of the pure solvent η_0 divided by the absolute temperature for solutions of NaBp and KBp, respectively. For NaBp in THF an increase of the linewidth is observed as the temperature increases. This means that the magnitude of the interaction parameters (\bar{A} , D and eQq/\hbar) increase with tempe-

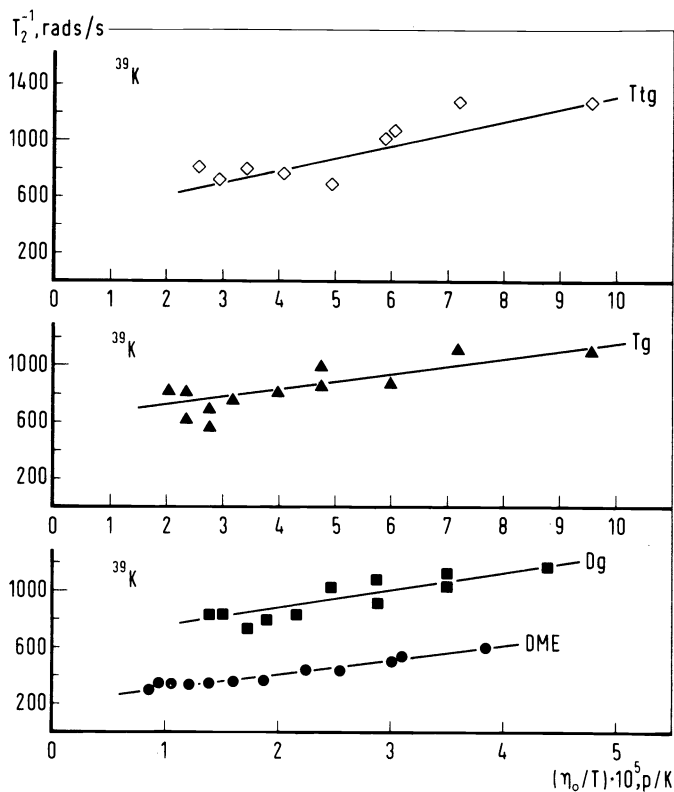


Fig. 4. ^{39}K NMR linewidths in rad/s as a function of the viscosity of the pure solvent divided by the absolute temperature for solutions of KBp in DME, Dg, Tg and Ttg.

CRYSTAL STRUCTURES OF NaBp.2Tg, KBp.2Ttg AND RbBp.2Ttg

In our efforts to prepare single crystals of aromatic anions we have investigated all combinations of alkali metals with biphenyl in seven different solvents, viz. THF, THF, 2-methyl-THF, DME, Dg, Tg and Ttg. Only four combinations gave rise to single crystals, namely LiBp in THF, NaBp in Tg, KBp in Ttg and RbBp in Ttg. The crystals of LiBp in THF crystallize in diamond-shaped plates and could reach dimensions of about $4 \times 15 \times 15$ mm. However, these crystals are very difficult to handle, due to the high volatility of the solvent molecules. In a non solvent-saturated atmosphere these crystals loose solvent molecules and subsequently decompose. This awkward circumstance does not occur in the crystals containing glyme molecules, although still one has to cope with the extreme sensitivity of the crystals to air and moisture. We were able to solve the crystal structures of NaBp.2Tg, KBp.2Ttg and RbBp.2Ttg. In Figure 5 stereoscopic views of the unit cell contents are given and Table 1 gives a compilation of the crystal data. Clearly all crystals can be characterized as solvent separated ion pairs. The alkali ion is spherically surrounded by two glyme molecules and coordinated to eight (NaBp) or ten oxygen atoms (KBp and RbBp). In our discussion on the NMR experiments on these systems in solution it was suggested that these solvent separated ion pairs also existed in solution (cf section: NMR EXPERIMENTS ON SOLUTIONS). It is gratifying that these structures are realized in the solid state and that owing to this a clearer view is generated about the concept of solvent separated ion pairs. Figure 5 illustrates that the biphenyl anions and the alkali glyme parts lie in separated regions of the unit cell. The arrangement of the biphenyl anions prevents a strong π - π interaction. The strongest interaction probably may occur in NaBp.2Tg, since the bc plane is rather densely occupied by biphenyl anions.

Since the molecular structures of KBp.2Ttg and RbBp.2Ttg have been published elsewhere (refs. 10 and 5, respectively), we will here focus our attention on the structural properties of NaBp.2Tg. The dihedral angle between the two phenyl rings amounts to 7.2° , while it was 9.4° in RbBp.2Ttg. In Figure 6 the bond distances and angles in the biphenyl anion are given. The shortened distance of the central C-C bond (1.435 \AA) as compared with the neutral molecule (1.51 \AA) increases the repulsion between the orthohydrogen atoms and may be responsible for the dihedral angle (neutral biphenyl is "planar" in the solid state)(13). The orthohydrogen repulsion expresses itself furthermore in the angles around the central bond,

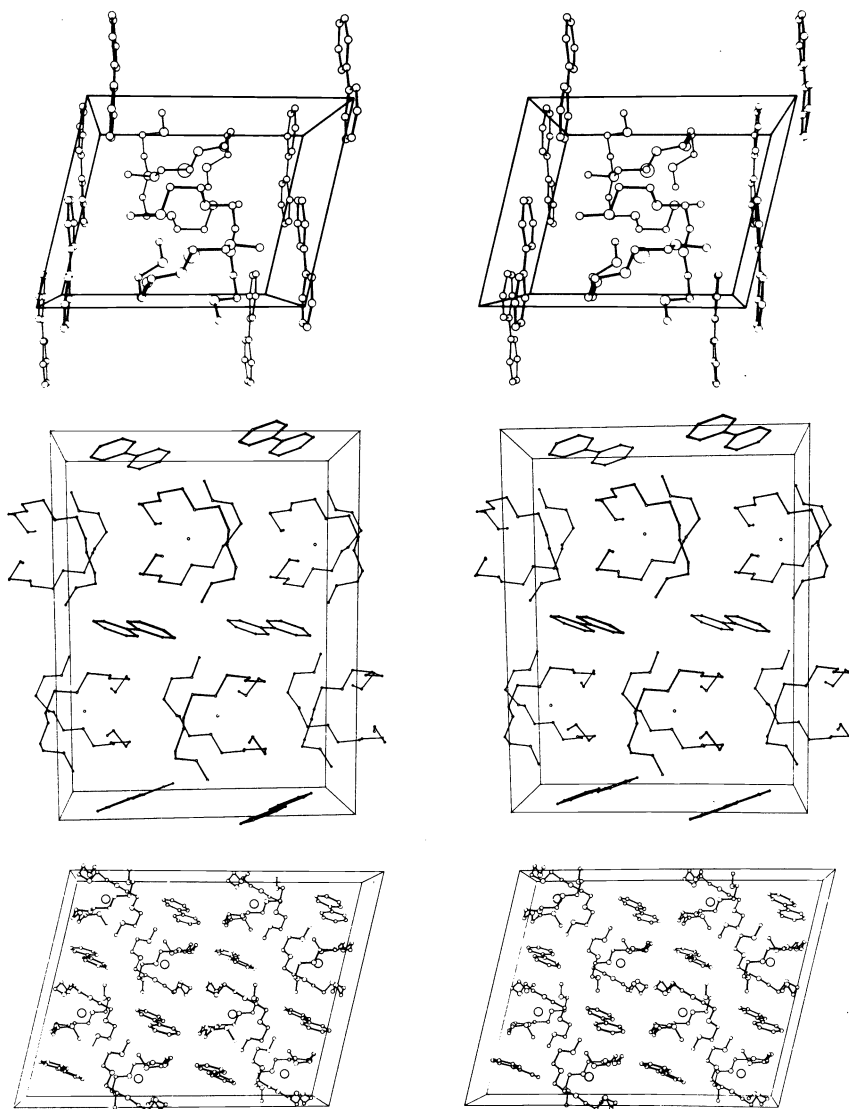


Fig. 5. Stereoscopic views of the unit cell for NaBp.2Tg along the b axis (top figure), for KBp.2Tg along the a axis (middle figure), for RbBp.2Tg along the b axis (bottom figure).

TABLE 2. Bond distances (in Å) and angles (in degrees) in the sodium triglyme part of NaBp.2Tg.

	smallest value	largest value	average value
Na-O	2.504	2.755	2.579
Triglyme molecules			
C-O	1.415	1.432	1.425
C-C	1.488	1.501	1.495
C-O-C	109.9	113.8	112.1
O-C-C	106.7	109.8	107.8

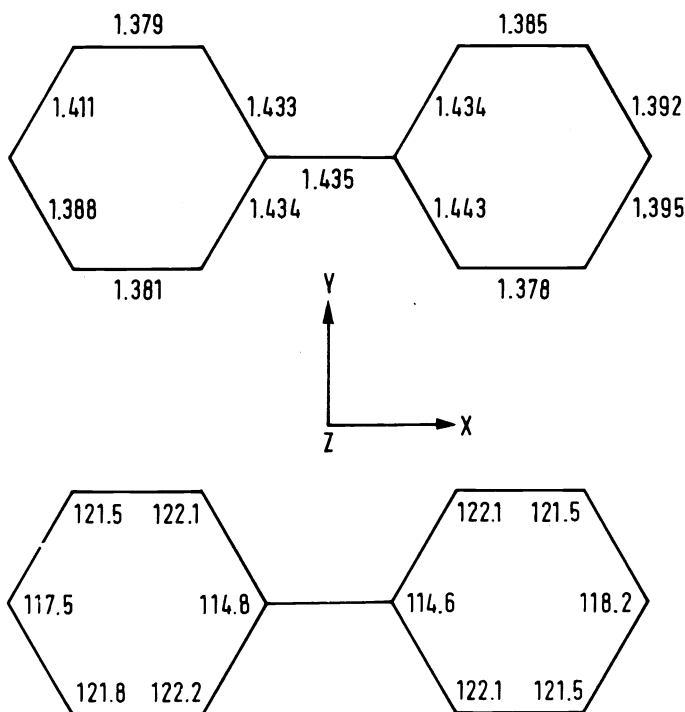


Fig. 6. Bond distances (in Å) and angles (in degrees) in the biphenyl anion part of NaBp.2Tg. Standard deviations are 0.005 Å or 0.4°.

which deviate significantly from 120°. In Table 2 bond distances and angles are given for the sodium triglyme part of NaBp.2Tg. Taking the average values for the alkali-oxygen distances for the three crystals under investigation and the Van der Waals radius of oxygen (1.40 Å) we calculated the Van der Waals radii of the alkali ions (column 4 of Table 3). They agree very well with ionic radii given by Gourary and Adrian (14), who corrected the values of Pauling (15).

TABLE 3. Average alkali-oxygen distances and alkali ionic radii (in Å).

distance	average value	Van der Waals oxygen radius	calculated alkali radius	Gourary and Adrian	Pauling
Na-O	2.58	1.40	1.18	1.17	0.95
K-O	2.93	1.40	1.53	1.49	1.33
Rb-O	3.02	1.40	1.62	1.63	1.48

If the central ions are regularly surrounded by the anions the critical ratios of the radii of cation and anion are 0.73 for eight coordination and 1.00 for 12 coordination (16). The relevant ratios in our crystals are: $r_{\text{Na}^+}/r_{\text{O}} = 0.83$, $r_{\text{K}^+}/r_{\text{O}} = 1.06$ and $r_{\text{Rb}^+}/r_{\text{O}} = 1.17$. Hence eight coordination for Na is feasible and ten coordination for K and Rb. The fact that single crystals of NaBp in Ttg cannot be prepared may arise from the too large diameter of the molecular cavity formed by the ten oxygen atoms. The central ion has then too much space, may move to one side and looses contact with the superfluous oxygen atoms. This may prevent the formation of the crystal. It is noteworthy that Smid and Grotens (17) were able to make single crystal of Na-tetraphenylborate (NaBPh₄) of composition NaBPh₄.2Tg. Since the crystal structure is yet unknown, it is not certain if all oxygen atoms are coordinated to the sodium ion. Single crystals could not be prepared for KBp and RbBp dissolved in Tg. Apparently too much space is left around these cations, which is energetically an unfavorable situation.

In conclusion it can be said that single crystals of biphenyl anions can only be found for very specific combinations of an alkali ion and solvent molecules. When solvation is studied not only the dielectric constant of the solvents and their ability to donate electrons to the cations are important, but also the number of chelating sites of the solvent molecules and steric factors.

MAGNETIC EXPERIMENTS ON SOLIDS

Susceptibility

Susceptibility measurements revealed that in the crystals of NaBp.2Tg and KBp.2Tg a ferromagnetic coupling exists and in RbBp.2Tg an antiferromagnetic coupling. From extrapolation of the high temperature points in the plots of χ^{-1} versus T for NaBp.2Tg and KBp.2Tg positive Weiss constants of $6.9 (\pm 0.5)$ and $7 (\pm 3)$ K, respectively were found (9). The susceptibility of RbBp.2Tg could be explained by a singlet-triplet dimer model, because in this crystal two nearest neighbor spins could be discerned at an average distance of 7.58 Å. Via a curve fitting procedure the singlet-triplet splitting was found to be $17 (\pm 2)$ cm⁻¹.

g-tensors

The crystals of NaBp.2Tg, KBp.2Tg and RbBp.2Tg all contain two magnetically different sites in the unit cell. The exchange coupling between the spins in the crystal averages out all intramolecular interactions. As a result a single exchange narrowed ESR line is observed. The resonance position of this line is the average value corresponding to the two inequivalent sites and the measured g tensor is the average of two tensors with equal principal values, but with different orientations.

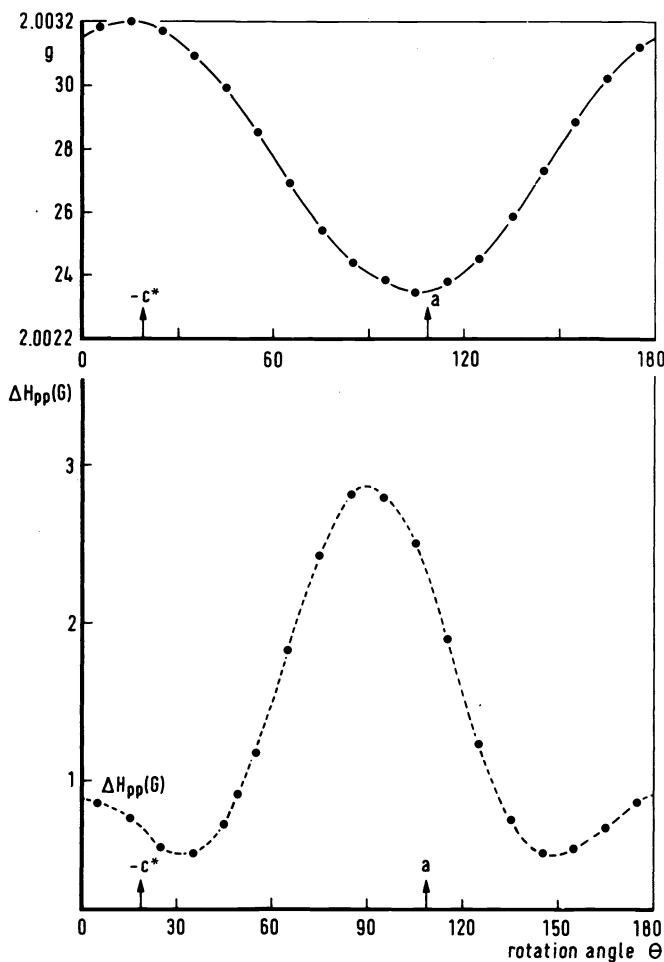


Fig. 7. The variation of the g value and the derivative linewidth ΔH_{pp} in G, as a function of the magnetic field, rotating in the ac plane.

In Figure 7 the g value is plotted for NaBp.2Tg as a function of the magnetic field in the ac plane. In the ac plane the principal directions of the g tensor are found 5° from the a and -c* direction, the corresponding principal values are 2.00231(1) and 2.00317(1). The third principal value is equal to 2.00280(1) and is found along the b axis. Using the known crystal structure the average g tensor can be transformed to the molecular g tensor. The method employed has been described in ref. 9 for the crystal of RbBp.2Tg. In Table 4 the

TABLE 4. Experimental and calculated values of the g tensor of the Bp anion in NaBp.2Tg, KBp.2Tg and RbBp.2Tg.

	exp.			calc.
	NaBp.2Tg	KBp.2Tg	RbBp.2Tg	
g_x	2.00330(1)	2.00339(1)	2.00334(2)	2.00328
g_y	2.00267(2)	2.00264(2)	2.00262(2)	2.00256
g_z	2.00231(2)	2.00227(2)	2.00230(2)	2.00238
g_{av}	2.00276(1)	2.00276(1)	2.00275(1)	2.00274
g_{iso}	2.002757(6)			

results of these transformations are listed for the three crystals considered. The principal directions of the g tensors are found parallel to the symmetry axes of the biphenyl anion (see Figure 6 for the assignment of the axes). As can be seen from Table 4 the three g tensors are nearly equal. Their average g value corresponds quite well with that measured for the "free" anion in solution. Influence, if any, of spin-orbit interaction of the alkali ion on the g tensor must be quite small. In the last column of Table 4 the g values, calculated with the theory of Stone (18), are listed, using for Stone's empirical parameter ($\gamma_1 - \gamma_2$) a value of -20×10^{-5} . Excellent agreement exists with the experimental values.

Structural information from g tensors

If the crystal structure is unknown it is not possible to derive from an average g tensor the molecular g tensor. In such situations g value measurements are of limited use. However, if certain conditions are fulfilled, it is still possible to obtain valuable structural information from the g value measurements. In an earlier publication (9) we reported the average g values of NaBp.2Tg. At that time the structure was unknown, and hence the molecular g tensor could not be derived. Making the supposition that the molecular g tensor of NaBp.2Tg would be equal to the molecular g tensor of RbBp.2Tg, we derived the rotation matrix, which relates the molecular g tensor to the average g tensor. From this rotation matrix the directions of the symmetry axes of the Bp anion with respect to the crystallographic axes could be derived. In Table 5 the result of this procedure is given: listed are

TABLE 5. Angles (in degrees) of the two fold axes x, y and z of the biphenyl anion with respect to the crystallographic axes a, b and c^* in NaBp.2Tg, as they were calculated from the average g tensor and from the crystal structure.

	From g tensor			From crystal structure		
	a	b	c^*	a	b	c^*
x	85.6	60	149.6	89.4	62.9	152.9
y	92.6	30	60.1	90	27.2	62.9
z	5.1	90	84.9	0.8	90.7	89.8

the angles between the symmetry axes and the crystallographic axes. Since the structure now is known, these angles can be compared with the angles, obtained from the crystal structure determination (see Table 5). It is gratifying to assess that within 5 degrees the angles agree with each other. Hence it can be concluded that measurement of g tensors can provide detailed structural information.

Linewidth

For the three crystals under investigation it was found that the linewidth of the exchange narrowed ESR line depended on the orientation of the crystal with respect to the magnetic field (5,10). In Figure 7 the behavior of the linewidth is shown for NaBp.2Tg, while the magnetic field is rotating in the ac plane. In this plane the two magnetically inequivalent sites become equivalent, so that there is no line broadening due to incomplete motional narrowing. The linewidth plotted is the peak to peak separation in the first derivative of the ESR absorption curve, which has a Lorentzian lineshape for all orientations. From the shape of the curve it is clear that the angular dependence of the linewidth is caused by the anisotropic dipole-dipole interaction between the electron spins. It has been shown by Anderson and Weiss (19) and by Van Vleck (20) that, if non-secular dipolar terms can be neglected, that $\omega_{\frac{1}{2}}$, the half width at half height is given by

$$\omega_{\frac{1}{2}} = \frac{\langle \Delta\omega^2 \rangle}{\omega_e} \quad (7)$$

where ω_e is the exchange frequency and $\langle \Delta\omega^2 \rangle$ the second moment in the absence of exchange. Van Vleck derived for the second moment

$$\langle \Delta\omega^2 \rangle = \frac{3}{4} S(S+1) \gamma^4 \hbar^2 \sum_k r_{jk}^{-6} (3\cos^2\theta_{jk} - 1)^2 \quad (8)$$

where r_{jk} = distance vector between the spins j and k . θ_{jk} = the angle between r_{jk} and the magnetic field.

It is clear that the observed linewidth quite closely follows the $(3\cos^2\theta - 1)^2$ relation. However, calculation of the sum in Eq.(8), yielded bad correspondence with the experimental curve. We are further investigating this problem (21).

Acknowledgement - The authors express their thanks to Prof. P.T. Manoharan for critical reading of the manuscript.

REFERENCES

1. H. Sadek and R.M. Fuoss, *J. Am. Chem. Soc.* **76**, 5897, 5905 (1954).
2. S. Winstein, E. Clippinger, A.H. Fainberg and G.C. Robinson, *J. Am. Chem. Soc.* **76**, 2597 (1954).
3. M. Szwarc, Ions and ion pairs in organic reactions Vol. 1,2, Wiley-Interscience, New York (1972).
4. G.W. Canters, A.A.K. Klaassen and E. de Boer, *J. Phys. Chem.* **74**, 3299 (1970).
5. J.J. Mooij, A.A.K. Klaassen, E. de Boer, H.M.L. Degens, Th.E.M. van den Hark and J.H. Noordik, *J. Am. Chem. Soc.* **98**, 680 (1976).
6. J.J. Brooks and G.D. Stucky, *J. Am. Chem. Soc.* **94**, 7333 (1972); J.J. Brooks, W. Rhine and G.D. Stucky, *ibid*, **94**, 7339 (1972); J.J. Brooks, W. Rhine and G.D. Stucky, *ibid*, **94**, 7346 (1972); W.E. Rhine, J. Davis and G.D. Stucky, *ibid*, **97** 2079 (1975); M. Walczak and G.D. Stucky, *ibid*, **98** 5531 (1976).
7. J.H. Noordik, Th.E.M. van den Hark, J.J. Mooij and A.A.K. Klaassen, *Acta Cryst.* **B30**, 833 (1974); J.H. Noordik, H.M.L. Degens and J.J. Mooij, *Acta Cryst.* **B31**, 2144 (1975); J.J. Mooij and E. de Boer, *Mol. Phys.* **32**, 113 (1976).
8. B.M.P. Hendriks, G.W. Canters, C. Corvaja, J.W.M. de Boer and E. de Boer, *Mol. Phys.* **20**, 193 (1971).
9. J.J. Mooij, A.A.K. Klaassen and E. de Boer, *Mol. Phys.* **32**, 879 (1976).
10. J.H. Noordik, J. Schreurs, R.O. Gould, J.J. Mooij and E. de Boer, *J. Phys. Chem.* May (1978).
11. J.H. Noordik, P.T. Beurskens, Th.E.M. van den Hark, J.M.M. Smits, *Acta Cryst.* (1979).
12. G.W. Canters and E. de Boer, *Mol. Phys.* **26**, 1185 (1973); G.W. Canters and E. de Boer, *ibid*, **27**, 665 (1974).
13. G.P. Charbonneau and Y. Delugeard, *Acta Cryst.* **B32**, 1420 (1976).
14. B.S. Gourary and F.J. Adrian, *Solid State Physics* **1k**, 127 (1960).
15. L. Pauling, The Nature of the Chemical bond 3rd ed., Cornell University Press, Ithaca (1960).
16. J.A.A. Ketelaar, De chemische binding p. 55, Elsevier, Amsterdam (1952).
17. J. Smid and A.M. Grotens, *J. Phys. Chem.* **77**, 2377 (1973).
18. A.J. Stone, *Mol. Phys.* **6**, 509 (1963); *ibid*, **7**, 311 (1964).
19. P.W. Anderson and P.R. Weiss, *Rev. Mod. Phys.* **25**, 269 (1953).
20. J.H. van Vleck, *Phys. Rev.* **74**, 1168 (1948).
21. J.E. Gulley, D. Hone, D.J. Scalapino and B.G. Silbernagel, *Phys. Rev.* **B3**, 1020 (1970).